

# The Lancet Microbe

## Experimental transmission studies of SARS-CoV-2 in fruit bats, ferrets, pigs and chickens --Manuscript Draft--

<b>Manuscript Number:</b>	THELANCETMICROBE-D-20-00091
<b>Article Type:</b>	Article (Original Research)
<b>Keywords:</b>	Sars-Cov-2; animal model; Rousettus fruit bat; ferret; pig; chicken
<b>Corresponding Author:</b>	Martin Beer Friedrich-Loeffler-Institut Greifswald-Insel Riems, GERMANY
<b>First Author:</b>	Kore Schlottau
<b>Order of Authors:</b>	Kore Schlottau Melanie Rissmann Annika Graaf Jacob Schön Julia Sehl Claudia Wylezich Dirk Höper Thomas C. Mettenleiter Anne Balkema-Buschmann Timm Harder Christian Grund Donata Hoffmann Angele Breithaupt Martin Beer
<b>Manuscript Region of Origin:</b>	GERMANY
<b>Abstract:</b>	<p><b>Background</b> A novel zoonotic SARS-related coronavirus emerged in China at the end of 2019. The novel SARS-CoV-2 became pandemic within weeks and the number of human infections and severe cases is increasing. The role of potential animal hosts is still understudied.</p> <p><b>Methods</b> We intranasally inoculated fruit bats ( <i>Rousettus aegyptiacus</i> ; n=9), ferrets (n=9), pigs (n=9) and chickens (n=17) with <math>10^5</math> TCID<sub>50</sub> of a SARS-CoV-2 isolate per animal. Animals were monitored clinically and for virus shedding. Direct contact animals (n=3) were included. Animals were humanely sacrificed for virological and immune-pathohistological analysis at different time points.</p> <p><b>Findings</b> Under these settings, pigs and chickens were not susceptible to SARS-CoV-2. All swabs as well as organ samples and contact animals remained negative for viral RNA, and none of the animals seroconverted. <i>Rousettus aegyptiacus</i> fruit bats experienced a transient infection, with virus detectable by RT-qPCR, immunohistochemistry (IHC) and in situ hybridization (ISH) in the nasal cavity, associated with rhinitis. Viral RNA was also identified in the trachea, lung and lung associated lymphatic tissue. One of three contact bats became infected. More efficient virus replication but no clinical signs were observed in ferrets with transmission to all direct contact animals. Prominent viral RNA loads of up to <math>10^4</math> viral genome copies/ml were detected in the upper respiratory tract. Mild rhinitis was associated with viral antigen detection in the respiratory and olfactory epithelium. Both fruit bats and ferrets developed SARS-CoV-2</p>

reactive antibodies reaching neutralizing titers of up to 1:1024.

Interpretation

Pigs and chickens could not be infected intranasally by SARS-CoV-2, whereas fruit bats showed characteristics of a reservoir host. Virus replication in ferrets resembled a subclinical human infection with efficient spread. These animals might serve as a useful model for further studies e.g. testing vaccines or antivirals.

Funding

Intramural funding of the German Federal Ministry of Food and Agriculture provided to the Friedrich-Loeffler-Institut.

Preprint not peer reviewed

# Experimental transmission studies of SARS-CoV-2 in fruit bats, ferrets, pigs and chickens

Kore Schlottau\*<sup>1</sup>, Melanie Rissmann\*<sup>2</sup>, Annika Graaf\*<sup>1</sup>, Jacob Schön\*<sup>1</sup>, Julia Sehl<sup>3</sup>, Claudia Wylezich<sup>1</sup>, Dirk Höper<sup>1</sup>, Thomas C. Mettenleiter<sup>4</sup>, Anne Balkema-Buschmann<sup>±,2</sup>, Timm Harder<sup>±,1</sup>, Christian Grund<sup>±,1</sup>, Donata Hoffmann<sup>±,1</sup>, Angele Breithaupt<sup>#,3</sup> and Martin Beer<sup>#,1</sup>

<sup>1</sup>Institute of Diagnostic Virology, Friedrich-Loeffler-Institut, Greifswald-Insel Riems, Germany

<sup>2</sup>Institute of Novel and Emerging Infectious Diseases, Friedrich-Loeffler-Institut, Greifswald-Insel Riems, Germany

<sup>3</sup>Department of Experimental Animal Facilities and Biorisk Management, Friedrich-Loeffler-Institut, Greifswald-Insel Riems, Germany

<sup>4</sup>Friedrich-Loeffler-Institut, Greifswald-Insel Riems, Germany

\*<sup>±</sup> Authors contributed equally to this work

# corresponding author

[Martin.beer@fli.de](mailto:Martin.beer@fli.de)

+49 38351 7 1200

[Angele.breithaupt@fli.de](mailto:Angele.breithaupt@fli.de)

+49 38351 7 1128

Lancet Microbe

Main Text: max 3500 words: 3579

Abstract: max 300 words: 300

References: max 30: 30

27 **Abstract**

28 **Background**

29 A novel zoonotic SARS-related coronavirus emerged in China at the end of 2019. The novel  
30 SARS-CoV-2 became pandemic within weeks and the number of human infections and severe  
31 cases is increasing. The role of potential animal hosts is still understudied.

32 **Methods**

33 We intranasally inoculated fruit bats (*Rousettus aegyptiacus*; n=9), ferrets (n=9), pigs (n=9) and  
34 chickens (n=17) with  $10^5$  TCID<sub>50</sub> of a SARS-CoV-2 isolate per animal. Animals were  
35 monitored clinically and for virus shedding. Direct contact animals (n=3) were included.  
36 Animals were humanely sacrificed for virological and immuno-pathohistological analysis at  
37 different time points.

38 **Findings**

39 Under these settings, pigs and chickens were not susceptible to SARS-CoV-2. All swabs as  
40 well as organ samples and contact animals remained negative for viral RNA, and none of the  
41 animals seroconverted. *Rousettus aegyptiacus* fruit bats experienced a transient infection, with  
42 virus detectable by RT-qPCR, immunohistochemistry (IHC) and in situ hybridization (ISH) in  
43 the nasal cavity, associated with rhinitis. Viral RNA was also identified in the trachea, lung and  
44 lung associated lymphatic tissue. One of three contact bats became infected. More efficient  
45 virus replication but no clinical signs were observed in ferrets with transmission to all direct  
46 contact animals. Mild rhinitis was associated with viral antigen detection in the respiratory and  
47 olfactory epithelium. Prominent viral RNA loads of up to  $10^4$  viral genome copies/ $\mu$ l were  
48 detected in the upper respiratory tract of both species, and both species developed SARS-CoV-  
49 2 reactive antibodies reaching neutralizing titers of up to 1:1024.

50 **Interpretation**

51 Pigs and chickens could not be infected intranasally by SARS-CoV-2, whereas fruit bats  
52 showed characteristics of a reservoir host. Virus replication in ferrets resembled a subclinical  
53 human infection with efficient spread. These animals might serve as a useful model for further  
54 studies e.g. testing vaccines or antivirals.

55 **Funding**

56 Intramural funding of the German Federal Ministry of Food and Agriculture provided to the  
57 Friedrich-Loeffler-Institut.

58 **Research in context**

59 Evidence before this study

60 While the first SARS-CoV pandemic could be controlled at an early stage before substantial  
61 spread occurred, SARS-CoV-2 has disseminated globally within weeks, and the number of  
62 infected humans continues to increase at alarming rates. Although the pandemic is driven by  
63 human-to-human transmission, the large number of infected humans also raises the question  
64 whether anthro-zoonotic infections occur by contact of infected humans with animals, which  
65 may lead to further spread and endemicity of SARS-CoV-2 in companion and farmed animals.  
66 However, contact with zoo and wild animals is also relevant, since bats are considered as  
67 reservoir hosts. Infection of ferrets and cats by SARS-CoV has been demonstrated  
68 experimentally and naturally. Field infections of pigs were also reported, while poultry did not  
69 appear to be affected. In addition to exploring potentially important epidemiological animal  
70 reservoirs, suitable animal models for testing vaccines and antiviral drugs are urgently required.  
71 For SARS-CoV, non-human primate and ferret models were used. First reports now indicate  
72 similar results for SARS-CoV-2. However, data on the susceptibility of bat species, as well as  
73 detailed analyzes including viral loads and histopathology of SARS-CoV-2 in ferrets and their  
74 contact animals are lacking. Furthermore, the first study on the inoculation of pigs and chickens  
75 requires confirmation and extension.

76 Added value of this study

77 In our study, four relevant animal species were intranasally inoculated: fruit bats, ferrets, pigs  
78 and chickens. Neither pigs (n = 9) nor chickens (n = 17) showed any signs of infection and none  
79 of the contact animals became infected. This is of particular importance for risk analysis in  
80 these farmed animals, which are kept in large numbers in contact with humans. Interestingly,  
81 this differs to the findings reported after infection of pigs with SARS-CoV. In contrast, the virus  
82 replicated in the upper respiratory tract of fruit bats, and was transmitted to contact animals.  
83 This indicates that fruit bats, which are kept and bred in captivity can serve as reservoir host  
84 model, but also emphasizes the risk to free-living bats e.g. in ecological bat protection  
85 programs. Finally, ferret infections resulted in a very high replication rate of SARS-CoV-2 in  
86 the nasal cavity, as confirmed by immunohistochemistry and in situ hybridization. The  
87 transmission to contacts was highly efficient and high virus titers were detected in the nasal  
88 cavity of contacts. We demonstrate by next-generation sequencing that no viral adaptations  
89 occurred during infection of ferrets with a human SARS-CoV-2 isolate. Our results suggest that

90 the ferret is a highly suitable model for testing vaccines and antiviral treatment for their effect  
91 on viral excretion and transmission.

92 Implications of all available evidence

93 Our results are in accordance with all so far available study results, indicating a negligible risk  
94 of anthro-zoonotic transmission to pigs and chickens, but relevant for bats and ferrets. Fruit  
95 bats show a different pattern of infection than ferrets, but both can serve as model animals.  
96 However, ferrets next to non-human primates, most closely mimic human infection and are  
97 therefore suggested as animal model for testing vaccines and antivirals.

98

99 **Introduction**

100 Coronaviruses are enveloped viruses with a large single-stranded RNA genome of positive  
101 polarity (ICTV; (1)). While numerous coronaviruses have been identified in animals or humans  
102 (2), two recent  $\beta$ -coronaviruses are remarkable: the Severe Acute Respiratory Syndrome  
103 coronavirus (SARS-CoV) (3, 4); and the Middle East Respiratory Syndrome coronavirus  
104 (MERS) (5, 6). Both viruses presumably originate from bats (7), but adapted to further animals  
105 like palm civets (8) or dromedary camels (6) from which sporadic or sustained spill-over  
106 infections occurred resulting in abundant (SARS-CoV) (9), or limited human-to-human  
107 infection chains (MERS-CoV) (10), which finally could be controlled.

108 Since the end of 2019, another SARS-CoV-related zoonotic  $\beta$ -coronavirus - Severe Acute  
109 Respiratory Syndrome coronavirus 2 (SARS-CoV-2) – has been spreading pandemically from  
110 Wuhan, China. As for SARS-CoV and MERS-CoV,  $\beta$ -coronaviruses very closely related to  
111 SARS-CoV-2 were found in bats (11, 12) and Pangolins (13). Whether the pandemic started by  
112 a direct spill-over transmission of the SARS-CoV-2 ancestor from bats to humans or via another  
113 intermediate mammalian host providing further adaptation to the human host, is still under  
114 debate.

115 Due to the zoonotic origin of SARS-CoV-2 from the likely bat reservoir, several questions  
116 concerning the susceptibility of animals arise: (i) susceptibility of putative reservoir hosts like  
117 bats, (ii) risk of possible anthro-zoonotic spill-over infections to farmed animals, and (iii)  
118 suitable animal models of human infection to study antivirals and vaccine prototypes. Viral  
119 receptor structure may be used as an important predictive factor of susceptibility: Recently it  
120 was shown, that SARS-CoV and SARS-CoV-2 employ the same receptor molecule, ACE2 (14),  
121 for contact with the receptor-binding-domain (RBD) of the spike (S) protein. Based on  
122 molecular studies the ACE2 proteins of human primates, pigs, cats and ferrets closely  
123 resembled the human ACE2 receptor. Therefore, these species may be susceptible to SARS-  
124 CoV-2 infection as has been shown for SARS-CoV and MERS-CoV (15, 16). During the last  
125 influenza A virus H1N1 pandemic in 2009, the virus was transmitted from humans to pigs, and  
126 is now endemic in pig holdings worldwide (17), posing a continuous risk of zoonotic spill-back  
127 infections. The potential impact of a SARS-CoV-2 infection of pigs therefore is very high. In  
128 this context, it is also very important to prove that chickens are not susceptible to SARS-CoV-  
129 2. Finally, bats as a major reservoir host of  $\beta$ -coronaviruses and especially SARS-CoV-related  
130 viruses (18) need to be further studied to better understand the viral replication, shedding,  
131 transmission or persistence in a putative reservoir host species.

132 Here, we intranasally inoculated fruit bats, ferrets, pigs and chickens with SARS-CoV-2 and  
133 investigated virus replication and shedding, the clinical course, pathohistological changes as  
134 well as transmission.

135

136

137

138



139 **Materials and methods**

140 Ethics

141 The animal experiments were evaluated and approved by the ethics committee of the State  
142 Office of Agriculture, Food safety, and Fishery in Mecklenburg – Western Pomerania (LALLF  
143 M-V: LVL MV/TSD/7221.3-2-010/18-12). All procedures were carried out in approved  
144 biosafety level 3 (BSL3) facilities.

145 Animals & study design

146 Twelve Egyptian fruit bats (*Rousettus aegyptiacus*, mixed sexes and ages, originating from the  
147 FLI breeding colony), twelve ferrets (*Mustela putorius*, female, nine-twelve month old,  
148 originating from the FLI breeding colony), twelve male pigs (*Sus scrofa domesticus*, nine weeks  
149 old; raised by BHZP GmbH (Dahlenburg, Germany)) and twenty chickens (*Gallus gallus*  
150 *domesticus* (white leghorn, five weeks old, mixed sexes, hatched from SPF-eggs (VALO  
151 BioMedia GmbH, Osterholz-Scharmbeck, Germany)) were used. Fruit bats as well as pigs were  
152 kept in groups of four and six in different cages and stables, respectively. Ferrets were kept  
153 altogether in one cage and chickens were kept in free run conditions with nests and perches. All  
154 animals were offered water ad-libitum, and were fed and checked for clinical scores daily and  
155 by video supervision during the 21-day study period. All animals tested negative for SARS-  
156 CoV-2 genome and antibodies prior to the experiment.

157 Nine fruit bats, ferrets and pigs were infected intranasally while the 17 chickens received oculo-  
158 oronasally  $10^5$  TCID<sub>50</sub> SARS-CoV-2 2019\_nCoV Muc-IMB-1 per animal (kindly provided by  
159 R. Woelfel, German Armed Forces Institute of Microbiology, Munich, Germany). The  
160 inoculum was administered to both nostrils using a pipette (fruit bats, ferrets and chickens) or  
161 an intranasal spraying device (pigs) (Teleflex Medical GmbH, Germany). To test viral  
162 transmission by direct contact, three naïve sentinel animals were added 24 hours post  
163 inoculation. Animals were monitored for body temperature (pigs, fruit bats, ferrets) and body  
164 weight (fruit bats, ferrets) throughout the experiment. Viral shedding was tested on nasal  
165 washes and rectal swabs (ferrets), oral swabs and pooled feces samples (fruit bats), nasal and  
166 rectal swabs (pigs) or oropharyngeal and cloacal swabs (chicken) on 2, 4, 8, 12, 16, and 21 days  
167 post infection (dpi). On day 4 (animals #1,#2), day 8 (animals #3,#4) and 12 dpi (animals  
168 #5,#6), two or three (chickens) inoculated animals of each species were sacrificed. All  
169 remaining animals, including the sentinels, were euthanized on day 21 pi (Fig. 1). All animals  
170 were subjected to autopsy. For virus detection and histopathology: nasal conchae, trachea, lung,

171 tracheobronchial lymph node (not for chicken), heart, liver, spleen, duodenum, colon/cecum,  
172 pancreas, kidney, adrenal gland, skeletal muscle, skin, brain were collected.

173 Further materials and methods

174 For details on virus, cells, virus titration, RNA extraction, RT-qPCR, next-generation  
175 sequencing, antibody detection, histopathology, immunohistochemistry and in-situ  
176 hybridization, please refer to the materials&methods section in the supplement.

177 Role of the funding source

178 The funder of the study had no role in study design, data collection, data analysis, data  
179 interpretation, or writing of the report. MB had full access to all the data in the study and had  
180 final responsibility for the decision to submit for publication.

181

182 **Results**

183 **Egyptian fruit bats**

184 No clinical signs (such as anorexia or respiratory signs), elevated temperatures, body weight  
185 loss or mortality were observed in any of the bats.

186 Oral virus shedding was observed in infected bats from 2 to 12 dpi, with one out of the three  
187 remaining infected bats still virus positive at 12 dpi (fruit bat #8), the other ones were sacrificed  
188 as scheduled on 4 and 8 dpi. Oral shedding was also detected in two out of three contact animals  
189 until 8 dpi (fruit bats #10 & #11, Fig 2A). Virus was isolated from one oral swab on day 2 pi  
190 ( $10^{1.75}$  TCID<sub>50</sub>/ml, fruit bat #8) (Fig 3A). Fecal shedding was observed in all three cages at 2  
191 and 4 dpi with Cq values ranging from 29.54 to 36.43 (data not shown). SARS-CoV-2 genome  
192 (Cq values between 23.16 and 38.97;  $1.96 \times 10^4$  to  $1.32 \times 10^1$  genome copies/ $\mu$ l RNA) was  
193 detected in the nasal epithelium in seven of nine infected bats sacrificed at 4, 8 and 21 dpi, with  
194 one animal each giving negative results at 8 and 12 dpi respectively. Interestingly, the nasal  
195 epithelium of one contact animal contained viral RNA on day 21 pi (Cq value 32.89; 3.12  
196 genome copies/ $\mu$ l RNA). At 4 dpi, genome was also detected in respiratory tissues (trachea  
197 (2/2), lung (1/2) and lung associated lymphatic tissue (2/2)) and at lower levels in heart, skin,  
198 duodenum and adrenal gland (one animal at 4 dpi) and in duodenum, skin and adrenal gland  
199 (one animal) on 8 dpi (Fig 2C). Virus could be cultivated from the trachea ( $10^{2.25}$  TCID<sub>50</sub>/ml)  
200 and the nasal epithelium ( $10^{1.75}$  TCID<sub>50</sub>/ml) of fruit bat #2 at 4 dpi. For all other RT-qPCR  
201 positive samples, cultivation of replicating virus was impossible.

202 SARS-CoV-2 reactive antibodies were observed in all inoculated bats by iIFA starting from 8  
203 dpi as well as in one contact bat (#10) on day 21 with titers  $\geq 16$ . Only a slight increase in  
204 antibody levels could be observed between day 8 and day 21 (with varying titers between 16  
205 and 64). Neutralizing antibodies could be detected in the same fruit bats with titers up to 64  
206 (Table 1A).

207 Necropsy revealed no pathological alterations in any of the inoculated or contact bats. At 4 dpi,  
208 minimal to mild rhinitis was found, with epithelial necrosis, edema, infiltrating lymphocytes  
209 and neutrophils, and intraluminal cellular debris (Fig 4A). Immunohistochemistry (IHC)  
210 revealed viral antigen, restricted to foci in the nasal respiratory epithelium and single cells of  
211 the non-respiratory, stratified epithelium (fruit bats #1,2; Fig. 4B,C), confirmed by in situ  
212 hybridization (ISH). Although viral antigen was absent at later time points, moderate rhinitis  
213 was detected at 8 dpi (fruit bats #3, #4), 12 dpi (fruit bat #6), and to a milder extent at 21 dpi  
214 (fruit bats #7, #11), indicating previous replication sites. Despite the detection of viral RNA by

215 RT-qPCR, no viral antigen was detectable in the lung. However, single infected animals at 4, 8  
216 and 12 dpi as well as one contact animal presented with interstitial, mixed cellular infiltrates  
217 and in one case also with perivascular lymphocytic cuffs (Table S.1, Fig. S.1A-C). Minimally  
218 increased numbers of alveolar macrophages were found at all time points. None of the other  
219 organs were found positive for viral antigen and no further relevant morphological changes  
220 were detected.

## 221 Ferrets

222 None of the ferrets showed clinical signs or loss of body weight during the study period. Body  
223 temperatures remained normal.

224 Viral shedding was detected in nasal washes in eight out of nine infected ferrets between day 2  
225 and day 8 pi with Cq values ranging from 21.77 to 36.35 ( $8.44 \times 10^3$  to 0.34 genome copies/ $\mu$ l  
226 RNA). Virus isolation was successful from nasal washes collected on days 2 pi (ferret #2,3,4:  
227  $10^{2.5} - 10^{2.875}$  TCID<sub>50</sub>/ml) and 4 pi (ferret #4;  $10^{2.75}$  TCID<sub>50</sub>/ml) (Fig. 3B). All three naïve ferrets  
228 were infected by direct contact to the other inoculated ferrets. The first RT-qPCR positive nasal  
229 wash sample in a contact ferret was observed on 8 dpi. Ferret #12 showed viral shedding on 8  
230 and 12 dpi (Cq values 37.03 and 28.59, respectively). Ferret #11 had positive results in nasal  
231 washes between day 12 and 21 pi (Cq values 37.39, 26.15 and 36.93) and ferret #10 on day 16  
232 and 21 pi (Cq values 28.04 and 30.00) (Fig. 2B). Analysis of the rectal swabs showed minor  
233 amounts of viral RNA in individual ferrets at singular time points with Cq values between 33.97  
234 and 38.45 (data not shown).

235 The two ferrets (ferret #1,#2) sacrificed at 4 dpi were RT-qPCR positive in different tissues  
236 (lung, muscle, skin, trachea, lung lymph node and colon) with the highest viral genome load in  
237 the nasal conchae (Cq values 24.31 and 26.21;  $1.93 \times 10^3 - 5.26 \times 10^2$  genome copies/ $\mu$ l RNA).  
238 The two ferrets euthanatized at 8 dpi (ferret #3,#4) were positive in the nasal conchae (Cq values  
239 34.77 and 21.57;  $1.61 - 1.21 \times 10^4$  genome copies/ $\mu$ l RNA). On 12 dpi, one of two ferrets was  
240 also positive in the nasal conchae (ferret #6, Cq value 29.26). The last three inoculated ferrets  
241 were sacrificed at 21 dpi. These animals showed only very weak RT-qPCR positivity in the  
242 cerebrum (ferret #7, Cq value 37.78) and in the caecum (ferret #9, Cq value 37.47). The three  
243 contact ferrets euthanized on the same day (21 dpi) were all positive in the nasal conchae (Cq  
244 values between 26.29 and 36.51). In addition, RT-qPCR positive samples were collected from  
245 muscle, lung, cerebrum, cerebellum and trachea tissue, which were all positive in ferret #10 and  
246 #11 whereas lung lymph node, skin and adrenal gland were only positive in one animal (Fig.  
247 2D).

248 Antibodies against SARS-CoV-2 were detected by iIFA from day 8 pi in all inoculated ferrets  
249 with varying titers (64 to 8192). One of three contact animals also showed high antibody titers  
250 (ferret #12, highest reactive serum dilution 8192), whereas the others remained negative.  
251 Neutralizing antibodies were observed in three inoculated ferrets (ferret #7 128; ferret #8 1024  
252 and ferret #9 1024 as the highest effective serum dilution) sacrificed on day 21 pi and one  
253 contact animal (ferret #12, 256) by VNT (Table 1B).

254 Post mortem examination did not identify relevant pathological alterations. At 4 dpi, viral  
255 antigen was associated with rhinitis, showing epithelial degeneration and necrosis, intraluminal  
256 cellular debris and mild inflammation (Fig. 4D-F). A more pronounced rhinitis developed at  
257 day 8 and 12 pi. At 21 dpi, rhinitis was only slightly detectable (ferret #7) or absent (ferret  
258 #8,#9). We also observed an antigen associated rhinitis in the contact ferrets (#10,#11). Viral  
259 antigen was detected in the nasal cavity at days 4 pi (ferret #1,#2), 8 pi (ferret #3), and 21 pi  
260 (contact ferret #10#11) in the nasal respiratory and olfactory epithelium. Remarkably, the  
261 olfactory epithelium of the vomero-nasal organ was affected (ferret #11; Fig. S2A-C). IHC  
262 results were confirmed by ISH (Fig. S3A-B). No viral antigen was identified in the lung. Single  
263 infected animals at days 4 and 8 pi and all contact animals showed interstitial, mixed cellular  
264 infiltrates and in some cases also perivascular lymphocytic cuffs (Table S1, Fig. S1D-F).  
265 Minimally increased numbers of alveolar macrophages were found at all time-points. None of  
266 the other organs was found positive for viral antigen, and no further relevant morphological  
267 alterations were detected.

#### 268 Pigs and chickens

269 No clinical signs, including elevated body temperatures, were observed in any of the 12 pigs or  
270 20 chickens. All collected samples were negative for SARS-CoV-2 genome. SARS-CoV-2  
271 reactive antibodies were not detected. Histopathology was inconspicuous (animals sacrificed at  
272 4, 8, and 12 dpi) or not performed on tissues obtained from animals sacrificed at 21 dpi. Three  
273 porcine cell lines (PK-15, SK-6 and ST) as well as embryonated chicken eggs inoculated with  
274 SARS-CoV-2 proved to be non-permissive (data not shown).

275 **Discussion**

276 Our study focused on four animal species, which are potentially relevant as models (fruit bats,  
277 ferrets) or could pose a risk as a viral reservoir following anthropo-zoonotic spill-over  
278 infections into food-producing animals (pigs, chickens).

279 Neither pigs (n = 9) nor chickens (n = 17) were susceptible to SARS-CoV-2 by intranasal or  
280 oculo-oronasal infection. All swabs as well as organ samples and contact animals (three animals  
281 in direct contact) remained negative for SARS-CoV-2 RNA and did not seroconvert. Non-  
282 permissiveness of chickens to SARS-CoV-2 infection parallel previous reports on the lack of  
283 susceptibility of chicken to SARS-CoV (20) and confirm recently reported results (21). We  
284 showed that this extends to embryonated chicken eggs, which are a classical substrate for  
285 isolation and propagation of a plethora of zoonotic viruses. The chicken data are also in  
286 agreement with studies on the chicken ACE2 receptor (22) that contains alterations in three of  
287 five critical residues (K31E; E35R, M82R). In contrast, similar predictions suggested that pigs  
288 as well as ferrets would likely be susceptible to SARS-CoV-2 due to their matching ACE2  
289 receptor-binding site (22). In contrast to such *in silico* predictions, our study as well as the report  
290 by Shi et al (21) ruled out any susceptibility of pigs by the intranasal inoculation route. We  
291 extend these findings further by showing non-permissiveness of three universal porcine cell  
292 lines (PK-15, SK-6 and ST cells).

293 On the other hand, we present here to our knowledge first data on the intranasal inoculation of  
294 nine *Rousettus aegyptiacus* fruit bats, which resulted in a transient infection in the respiratory  
295 tract and virus shedding. SARS-CoV-2 genome could be detected by RT-qPCR in nasal  
296 conchae, trachea, lung and lung lymph node in fruit bat #1 and fruit bat #2 as well as in skin  
297 and duodenum of fruit bat #2, dissected on day 4 pi (Fig. 2C). Infectious virus was isolated  
298 from nasal conchae and trachea tissues from the same animal. Virus shedding was detectable  
299 by RT-qPCR in oral swabs up to day 12 pi, but infectious virus could only be isolated from fruit  
300 bat #2 at 2 dpi (Fig 2A and 3A). In total, seven out of nine inoculated fruit bats had viral genome  
301 in their nasal cavity, as confirmed by IHC and ISH at 4 dpi. Rhinitis was the detectable lesion  
302 associated with presence of viral antigen, mainly in the respiratory epithelium. Despite the  
303 absence of viral antigen at later time points, rhinitis was still identifiable, indicating earlier  
304 replication sites. Some infected animals as well as contact fruit bat #10 presented with mild  
305 inflammation in the lung. Its occurrence and significance should be addressed in future studies,  
306 because no lesion-associated antigen was detectable. Starting from 8 dpi, a weak immune-  
307 response developed as demonstrated in iIFA and VNT. The virus was transmitted to one out of

308 the three naïve contact fruit bats (fruit bat #10). The other two naïve contact animals remained  
309 seronegative. Interestingly, in fruit bat #10 an early pregnancy was determined during necropsy.  
310 Several studies show a higher virus detection rate in bats during the reproductive phase,  
311 probably due to the associated immunosuppression (23).  $\beta$ -coronaviruses were shown to infect  
312 a variety of bat species with limited clinical signs even during active virus shedding (24).  
313 Moreover, low antibody titers are typical for bats (25). Although Egyptian fruit bats express  
314 ACE2 in the intestine and respiratory tract, an earlier study revealed very limited evidence of  
315 virus replication and seroconversion after infection with SARS-like coronaviruses, however,  
316 serum samples of some of these bats, collected prior to the infection, turned out to be already  
317 reactive with SARS S or N proteins (26). In the present study, SARS-CoV-2 transiently  
318 replicated in particular in the respiratory epithelium as shown by RT-qPCR, IHC and ISH. Our  
319 data suggest that intranasal infection of *Rousettus aegyptiacus* could reflect reservoir host  
320 status. Furthermore, we demonstrate that bat-to-bat transmission is possible. Consequently, bats  
321 are at risk of being infected anthro-po-zoonotically by SARS-CoV-2. It is therefore highly  
322 recommended, that during the pandemic, all contacts to bats, e.g. during research programs or  
323 ecological analyses should be avoided.

324 SARS-CoV-2 replicated most efficiently in ferrets. Eight of nine intranasally infected ferrets  
325 shed virus between day 2 and 8 pi. Viral genome was detected by RT-qPCR in nasal washes  
326 and infectious virus isolated from two animals at 2 and 4 dpi (Fig. 2B and 3B). Only ferret #5  
327 remained RT-qPCR negative during the observation period and developed only a weak iIFA  
328 titer. All other inoculated ferrets showed increasing SARS-CoV-2 reactive antibodies starting  
329 from day 8 pi. In general, the measured antibody levels were much higher in ferrets than in bats  
330 (Table 1), indicating a more prominent virus dissemination in the infected animals. For iIFA,  
331 this might also be explained by the use of different secondary antibodies. Neutralizing  
332 antibodies were only detected at later time points (21 dpi), but also with high titers of up to  
333 1024 in ferrets, while we detected neutralizing antibodies in bats from day 8 dpi at comparably  
334 low titers of 16 – 64 (Table 1B). This might represent a reservoir host infection, which deserves  
335 more detailed analysis in future studies.

336 SARS-CoV-2 was efficiently transmitted to three naïve ferrets by direct contact. In those  
337 animals, viral RNA was present in nasal washes starting from day 12 pi and detected by RT-  
338 qPCR mostly in the nasal conchae, but also lung, trachea, lung lymph node or cerebrum and  
339 cerebellum (Fig. 2D). Viral antigen within the upper respiratory tract was confirmed by strong  
340 positive IHC and ISH in the nasal cavity. In the case of SARS-CoV, the virus was found to  
341 replicate in the upper and lower respiratory tract, and the animals developed no or mild clinical

342 disease characterized by nasal discharge, sneezing and fever (27). We also used high-  
343 throughput sequencing to analyze the complete genome of the used virus inoculum as well of  
344 samples from the inoculated ferrets. Complete sequence identity demonstrates that the virus did  
345 not adapt during ferret inoculation and that no additional mutations were required for an  
346 efficient infection of these animals with a human SARS-CoV-2 isolate.

347 Our results are in line with two recent reports that were also able to show productive SARS-  
348 CoV-2 infection of ferrets with no, or only mild clinical signs (21, 28). However, histopathology  
349 and tissue tropism data were very limited in both studies. Our report adds important detailed  
350 histopathology substantiating the restriction of the main SARS-CoV-2 replication site to the  
351 nasal cavity. Presence of viral antigen in the nasal respiratory and olfactory epithelium,  
352 including the vomero-nasal organ, was associated with rhinitis. Interestingly, the lesions were  
353 still present at later time points despite absence of viral antigen. Nevertheless, no viral antigen  
354 was identified in the lung, although several animals showed pulmonary inflammation.

355 In general, RT-qPCR detected viral genome in a significantly broader spectrum of tissues as  
356 IHC. The differences could be explained by (i) a higher sensitivity of RT-qPCR, (ii) the  
357 restriction of labelling to cell associated antigen whereas RT-qPCR detects viral RNA in blood,  
358 secretions and excretions (i.e. tracheal and bronchial mucus, saliva on the fur), and not least  
359 (iii) viral antigen was found in restricted foci of the nasal cavity only, that might be missed in  
360 tissue sections although several areas have been analyzed. Although less sensitive, IHC is an  
361 excellent tool to localize and identify infected target cells. To avoid cross contamination at  
362 necropsy, instruments were washed in sodium hypochlorite-based reagents after each tissue  
363 sample. Numerous extraction controls were executed and questionable results were confirmed  
364 by a second RT-qPCR assay. Therefore, we assume that our RT-qPCR results are highly  
365 reliable. Testing a broader tissue spectrum, including salivary glands, the lower urinary tract,  
366 full gastrointestinal tract and the cerebrospinal fluid will help to increased understanding of the  
367 source of viral RNA in secretions, excretions as well as in the brain.

368 In summary, farmed animals like chickens and pigs were resistant against intranasal SARS-  
369 CoV-2 inoculation under our experimental conditions. This is relevant for risk assessment and  
370 epidemiology of the infection. Furthermore, our study demonstrated that ferrets and *Rousettus*  
371 fruits bats could be productively infected. Especially SARS-CoV-2 infection in ferrets, which  
372 resembles a mild infection of humans, might serve as a useful animal model for testing  
373 prototypic COVID-19 vaccines and antivirals.



374 **Acknowledgment**

375 The authors are very grateful to Roman Wölfel (German Armed Forces Institute of  
376 Microbiology) for providing the SARS-CoV-2 isolate used in this study. We thank Bernd  
377 Köllner for generating the anti-bat monoclonal antibody. We also acknowledge Mareen Lange,  
378 Christian Korthase, Silvia Schuparis, Gabriele Czerwinski and Patrick Zitzow for their  
379 excellent technical assistance and Frank Klipp, Doreen Fiedler, Harald Manthei, René Siewert,  
380 Christian Lipinski, Ralf Henkel and Dominique Lux for their excellent support in the animal  
381 experiments.

382 **Author's contribution**

383 KS, MR, AG, JS, DHo, ABB, TH and ChG performed the animal experiments. KS; MR; AG  
384 and JS did molecular, serological and classical virological analyses. AB and JuS did animal  
385 necropsies, AB did histopathology, immunohistochemistry and in situ hybridization analysis.  
386 DHö, CW and BH added sequencing and quantification data. KS; AG, DHo, TH, TM, ABB  
387 and MB designed the study. KS; MR; AG; AB and MB wrote the manuscript. All authors  
388 critically evaluated and approved the manuscript.

389

390 **Declaration of Interests**

391 All authors declare no competing interest.

392

393 **References**

- 394 1. Masters PS, Perlmen S. Fields Virology: Chaper 28: Coronaviridae. In: Knipe DM, Howley PM,  
395 eds. 2013;Philadelphia: Lippincott Williams & Wilkins:825-58.
- 396 2. Fehr AR, Perlman S. Coronaviruses Methods and Protocols: Coronaviruses: An Overview of  
397 Their Replication and Pathogenesis. In: Maier HJ, Bickerton E, Britton P, eds. 2015;Springer  
398 Protocols:1-27.
- 399 3. Tsang KW, Ho PL, Ooi GC, Yee WK, Wang T, Chan-Yeung M, et al. A cluster of cases of severe  
400 acute respiratory syndrome in Hong Kong. The New England journal of medicine. 2003;348(20):1977-  
401 85.
- 402 4. Peiris JSM, Lai ST, Poon LLM, Guan Y, Yam LYC, Lim W, et al. Coronavirus as a possible cause  
403 of severe acute respiratory syndrome. Lancet. 2003;361(9366):1319-25.
- 404 5. Zaki AM, van Boheemen S, Bestebroer TM, Osterhaus ADME, Fouchier RAM. Isolation of a  
405 Novel Coronavirus from a Man with Pneumonia in Saudi Arabia. New Engl J Med. 2012;367(19):1814-  
406 20.
- 407 6. Haagmans BL, Al Dhahiry SHS, Reusken CBEM, Raj VS, Galiano M, Myers R, et al. Middle East  
408 respiratory syndrome coronavirus in dromedary camels: an outbreak investigation. Lancet Infectious  
409 Diseases. 2014;14(2):140-5.
- 410 7. Li WD, Shi ZL, Yu M, Ren WZ, Smith C, Epstein JH, et al. Bats are natural reservoirs of SARS-  
411 like coronaviruses. Science. 2005;310(5748):676-9.
- 412 8. Song HD, Tu CC, Zhang GW, Wang SY, Zheng K, Lei LC, et al. Cross-host evolution of severe  
413 acute respiratory syndrome coronavirus in palm civet and human. Proceedings of the National  
414 Academy of Sciences of the United States of America. 2005;102(7):2430-5.
- 415 9. Cherry JD, Krogstad P. SARS: the first pandemic of the 21st century. *Pediatr Res*.  
416 2004;56(1):1-5.
- 417 10. Drosten C, Meyer B, Muller MA, Corman VM, Al-Masri M, Hossain R, et al. Transmission of  
418 MERS-Coronavirus in Household Contacts. New Engl J Med. 2014;371(9):828-35.
- 419 11. Zhou P, Yang XL, Wang XG, Hu B, Zhang L, Zhang W, et al. A pneumonia outbreak associated  
420 with a new coronavirus of probable bat origin. *Nature*. 2020.
- 421 12. Wu F, Zhao S, Yu B, Chen YM, Wang W, Song ZG, et al. A new coronavirus associated with  
422 human respiratory disease in China. *Nature*. 2020;579(7798):265-+.
- 423 13. Zhang T, Wu Q, Zhang Z. Probable Pangolin Origin of SARS-CoV-2 Associated with the COVID-  
424 19 Outbreak. *Curr Biol*. 2020;30(7):1346-51 e2.
- 425 14. Hoffmann M, Kleine-Weber H, Schroeder S, Kruger N, Herrler T, Erichsen S, et al. SARS-CoV-2  
426 Cell Entry Depends on ACE2 and TMPRSS2 and Is Blocked by a Clinically Proven Protease Inhibitor.  
427 *Cell*. 2020.
- 428 15. Gretebeck LM, Subbarao K. Animal models for SARS and MERS coronaviruses. *Current*  
429 *opinion in virology*. 2015;13:123-9.
- 430 16. Chen W, Yan M, Yang L, Ding B, He B, Wang Y, et al. SARS-associated coronavirus transmitted  
431 from human to pig. *Emerging infectious diseases*. 2005;11(3):446-8.
- 432 17. Novel Swine-Origin Influenza AVIT, Dawood FS, Jain S, Finelli L, Shaw MW, Lindstrom S, et al.  
433 Emergence of a novel swine-origin influenza A (H1N1) virus in humans. *The New England journal of*  
434 *medicine*. 2009;360(25):2605-15.
- 435 18. Wang LF, Shi ZL, Zhang SY, Field H, Daszak P, Eaton BT. Review of bats and SARS. *Emerging*  
436 *infectious diseases*. 2006;12(12):1834-40.
- 437 19. Belser JA, Katz JM, Tumpey TM. The ferret as a model organism to study influenza A virus  
438 infection. *Dis Model Mech*. 2011;4(5):575-9.
- 439 20. Swayne DE, Suarez DL, Spackman E, Tumpey TM, Beck JR, Erdman D, et al. Domestic poultry  
440 and SARS coronavirus, southern China. *Emerging infectious diseases*. 2004;10(5):914-6.
- 441 21. Shi J, Wen Z, Zhong G, Yang H, Wang C, Liu R, et al. Susceptibility of ferrets, cats, dogs, and  
442 different domestic animals to SARS-coronavirus-2. *Science*. 2020.

- 443 22. Wan YS, Shang J, Graham R, Baric RS, Li F. Receptor Recognition by the Novel Coronavirus  
444 from Wuhan: an Analysis Based on Decade-Long Structural Studies of SARS Coronavirus. *Journal of*  
445 *virology*. 2020;94(7).
- 446 23. Drexler JF, Corman VM, Wegner T, Tateno AF, Zerbinati RM, Gloza-Rausch F, et al.  
447 Amplification of Emerging Viruses in a Bat Colony. *Emerging infectious diseases*. 2011;17(3):449-56.
- 448 24. Shi ZL, Hu ZH. A review of studies on animal reservoirs of the SARS coronavirus. *Virus*  
449 *research*. 2008;133(1):74-87.
- 450 25. Schountz T, Baker ML, Butler J, Munster V. Immunological Control of Viral Infections in Bats  
451 and the Emergence of Viruses Highly Pathogenic to Humans. *Front Immunol*. 2017;8.
- 452 26. van Doremalen N, Schafer A, Menachery VD, Letko M, Bushmaker T, Fischer RJ, et al. SARS-  
453 Like Coronavirus WIV1-CoV Does Not Replicate in Egyptian Fruit Bats (*Rousettus aegyptiacus*).  
454 *Viruses*. 2018;10(12).
- 455 27. Enkirch T, von Messling V. Ferret models of viral pathogenesis. *Virology*. 2015;479:259-70.
- 456 28. Kim YI, Kim SG, Kim SM, Kim EH, Park SJ, Yu KM, et al. Infection and Rapid Transmission of  
457 SARS-CoV-2 in Ferrets. *Cell Host Microbe*. 2020.
- 458 29. Wylezich C, Papa A, Beer M, Hoper D. A Versatile Sample Processing Workflow for  
459 Metagenomic Pathogen Detection. *Scientific reports*. 2018;8(1):13108.
- 460 30. Corman VM, Landt O, Kaiser M, Molenkamp R, Meijer A, Chu DKW, et al. Detection of 2019  
461 novel coronavirus (2019-nCoV) by real-time RT-PCR. *Eurosurveillance*. 2020;25(3):23-30.

463

464

465

466 **Tables**

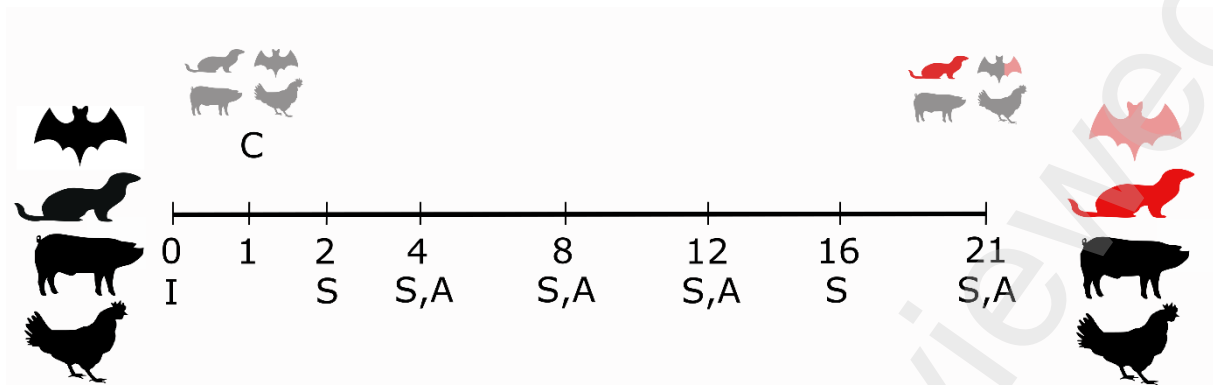
467 Table 1: Serological evidence of SARS-CoV-2 infection in A) fruit bats and B) ferrets.

A)	iIFA	VNT
fruit bat #1, day 4	< 1:16	< 1:16
fruit bat #2, day 4	< 1:16	< 1:16
fruit bat #3, day 8	<b>1:16</b>	<b>1:32</b>
fruit bat #4, day 8	<b>1:16</b>	<b>1:32</b>
fruit bat #5, day 12	<b>1:16</b>	<b>1:32</b>
fruit bat #6, day 12	<b>1:32</b>	<b>1:16</b>
fruit bat #7, day 21	<b>1:64</b>	<b>1:64</b>
fruit bat #8, day 21	<b>1:32</b>	<b>1:32</b>
fruit bat #9, day 21	<b>1:64</b>	<b>1:32</b>
fruit bat #10, day 21	<b>1:16</b>	<b>1:16</b>
fruit bat #11, day 21	< 1:16	< 1:16
fruit bat #12, day 21	< 1:16	< 1:16
B)	iIFA	VNT <sup>468</sup>
ferret #1, day 4	< 1:16	< 1:16 <sup>469</sup>
ferret #2, day 4	< 1:16	< 1:16
ferret #3, day 8	<b>1:128</b>	< 1:16 <sup>470</sup>
ferret #4, day 8	<b>1:512</b>	< 1:16
ferret #5, day 12	<b>1:64</b>	< 1:16 <sup>471</sup>
ferret #6, day 12	<b>1:4096</b>	< 1:16 <sup>472</sup>
ferret #7, day 21	<b>1:4096</b>	<b>1:128</b>
ferret #8, day 21	<b>1:8192</b>	<b>1:1024</b> <sup>473</sup>
ferret #9, day 21	<b>1:4096</b>	<b>1:1024</b> <sup>474</sup>
ferret #10, day 21	< 1:16	< 1:16
ferret #11, day 21	< 1:16	< 1:16 <sup>475</sup>
ferret #12, day 21	<b>1:8192</b>	<b>1:256</b> <sup>476</sup>

477

478

479 **Figures**



480

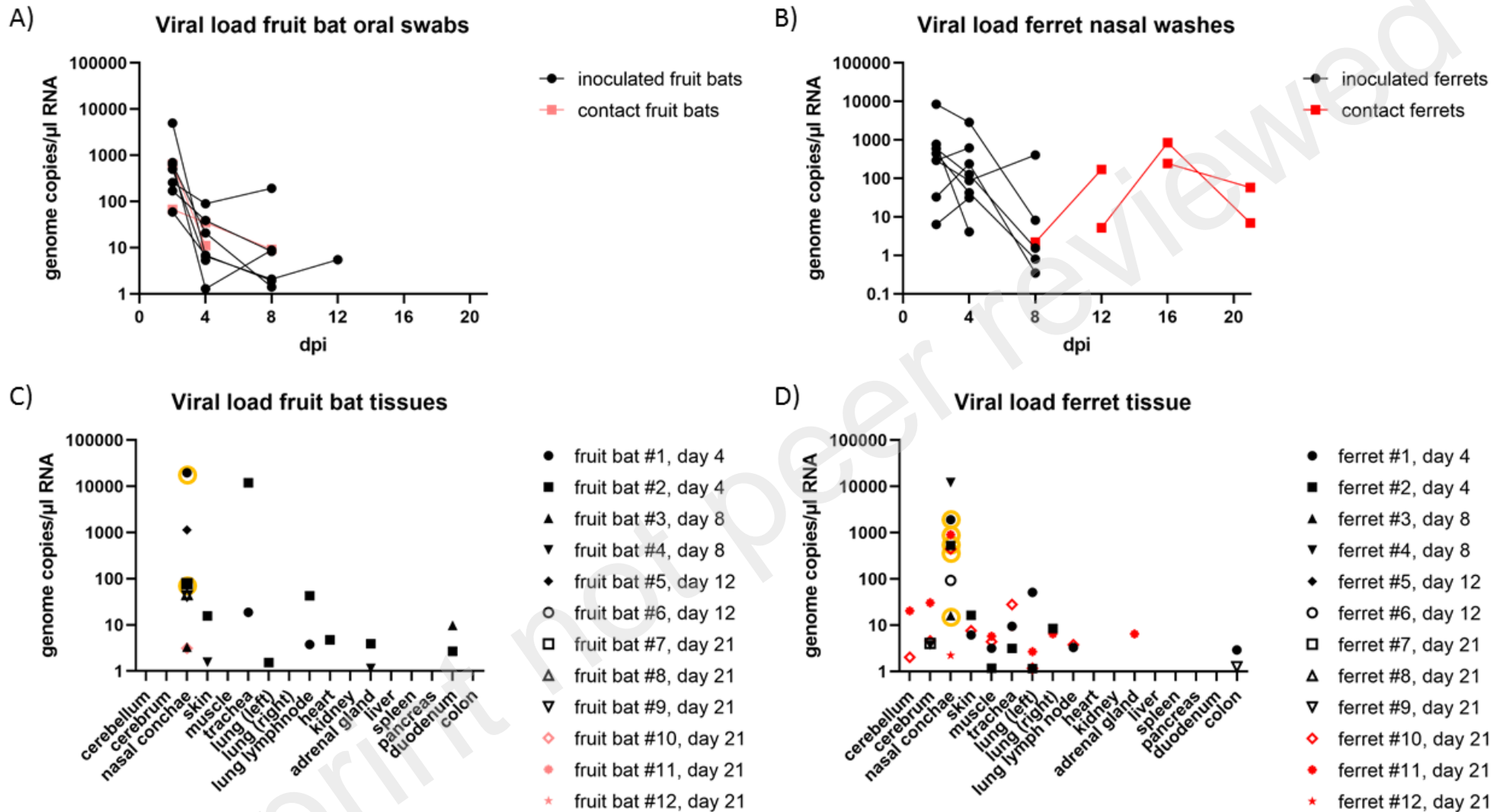
481

482 I - infection; C - contact animals; S - swabbing; A - Autopsy

483

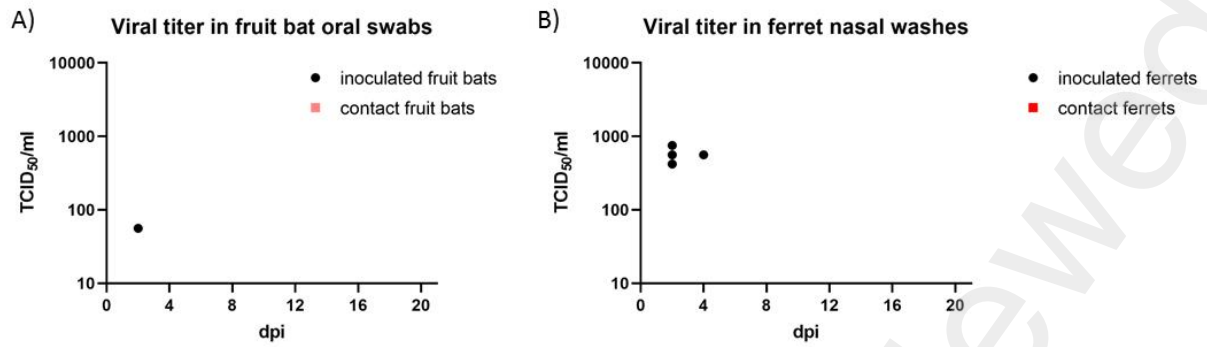
484 **Figure 1: Outline of the *in vivo* experiments with an observation period of 21 days.**

485 Procedure of the trials with fruit bats, ferrets, domestic pigs and chickens are shown. Black-  
486 colored animals (n=9 for each species, except chickens n=17) were inoculated intranasally (or  
487 oculo-oronasally for chicken) with  $10^5$  TCID<sub>50</sub>; grey animals (n=3 for each species) depict  
488 direct contact animals associated after day 1 post inoculation; black- and grey-colored animals  
489 on the right were found not susceptible; red animals became infected and showed strong viral  
490 shedding; rose/pink animals were infected but displayed only minute shedding of virus.



491

492 **Figure 2: SARS-CoV-2 viral genome loads in A) oral swabs of fruits bats, B) nasal washes of ferrets, tissues collected from C) fruit bats and D) ferrets**  
 493 **experimentally infected with SARS-CoV-2 and the contact animals, respectively.** Genome copies per  $\mu$ l RNA template were calculated based on a quantified  
 494 standard RNA. Red-colored animals became infected and showed strong viral shedding; rose/pink animals were infected but displayed only minute shedding of  
 495 virus. Organs with positive IHC results were marked with an orange ring.

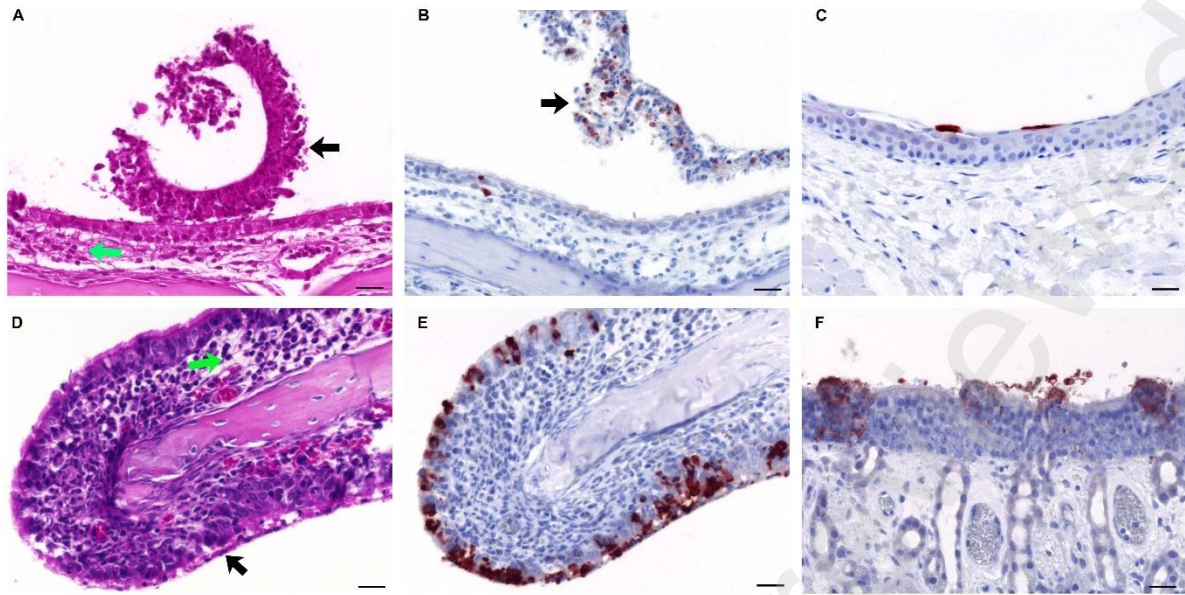


496

497 **Figure 3: Shedding of infectious SARS-CoV-2 in A) fruit bat oral swabs and B) ferret**  
 498 **nasal washes.** Given are TCID<sub>50</sub>/ml values for every day with a RT-qPCR positive result. All  
 499 other samples were <10<sup>1</sup>TCID<sub>50</sub>/ml for fruit bats or <10<sup>2.5</sup>TCID<sub>50</sub>/ml for ferrets.

500

501



502

503 **Figure 4. SARS-CoV-2 associated rhinitis and antigen detection at day 4 pi in a bat (A-C)**

504 **and a ferret (D-F).** (A) Bat, rhinitis, with intraluminal debris (black arrow), slight mucosal

505 edema and minimal inflammation (green arrow), (B) Bat, nasal respiratory epithelium,

506 intralesional viral antigen mainly within intraluminal debris, (C) Bat, non-respiratory

507 epithelium, with single antigen positive cells, no inflammation. (D) Ferret, rhinitis, with

508 degeneration and necrosis of the respiratory epithelium (black arrow), slight mucosal edema

509 and numerous infiltrates (green arrow), (E) Ferret, nasal respiratory epithelium, intralesional,

510 abundant viral antigen, (F) Ferret, olfactory epithelium, multifocal, intralesional viral antigen

511 (A, D) Histopathology, H&E stain, bar 20  $\mu\text{m}$  (B, C, E, F) Immunohistochemistry, ABC

512 method, AEC chromogen (red-brown), Mayer's hematoxylin counter stain (blue), bar 20  $\mu\text{m}$ .

513

514

515



516 **Supplementary**

517 **Supplementary Material & Methods**

518 **Virus and cells**

519 SARS-CoV-2 isolate 2019\_nCoV Muc-IMB-1 was kindly provided by German Armed Forces  
520 Institute of Microbiology (Munich, Germany). The complete sequence of this isolate is  
521 available through GISAID under the accession ID\_EPI\_ISL\_406862 and name “hCoV-  
522 19/Germany/BavPat1/2020”. The virus was propagated once in Vero E6 in a mixture of equal  
523 volumes of Eagle MEM (Hanks’ balanced salts solution) and Eagle MEM (Earle’s balanced  
524 salts solution) supplemented with 2mM L-Glutamine, nonessential amino acids, adjusted to 850  
525 mg/L, NaHCO<sub>3</sub>, 120 mg/L sodium pyruvate, 10% fetal bovine serum (FBS), pH 7.2. No  
526 contaminants were detected within the virus stock preparation and the sequence identity of the  
527 passaged virus (study accession number: PRJEB37671) was confirmed by metagenomics  
528 analysis employing previously published high throughput sequencing procedures using  
529 Illumina MiSeq sequencing (29). The virus was harvested after 72h, titrated on Vero E6 cells  
530 and stored at -80°C until further use.

531 **RNA extraction and detection of SARS-CoV-2**

532 Total RNA was extracted from oral, nasal and rectal samples, nasal washes, fecal samples and  
533 tissue samples collected at different time points using the NucleoMagVet kit  
534 (Macherey&Nagel, Düren, Germany) according to the manufacturer’s instructions. Tissue  
535 samples were homogenized in 1 ml cell culture medium and a 5 mm steel bead in a TissueLyser  
536 (Qiagen, Hilden, Germany). Fecal samples were vortexed in sterile NaCl and the supernatant  
537 was sterile filtered (22 µm) after centrifugation. Swab samples were transferred into 0.5-1 ml  
538 of serum-free tissue culture media and further processed after 30 min shaking.

539 SARS-CoV-2 RNA was detected by the “E-gene Sarbeco FAM” published by Corman et al.  
540 (30). The RT-qPCR reaction was prepared using the AgPath-ID-One-Step RT-PCR kit (Thermo  
541 Fisher Scientific, Waltham, Massachusetts, USA) in a volume of 12.5 µl including 1 µl of E-  
542 gene Sarbeco FAM mix, 1 µl of β-Actin-mix2-HEX as internal control) and 2.5 µl of extracted  
543 RNA. The reaction was performed for 10 min at 45°C for reverse transcription, 5 min at 95°C  
544 for activation, and 42 cycles of 15 sec at 95°C for denaturation, 20 sec at 57°C for annealing  
545 and 30 sec at 72°C for elongation. Fluorescence was measured during the annealing phase. All  
546 RT-qPCRs were performed on a BioRad real-time CFX96 detection system (Bio-Rad,  
547 Hercules, USA). Absolute quantification was done using a standard quantified by the QX200

548 Droplet Digital PCR System in combination with the 1-Step RT-ddPCR Advanced Kit for  
549 Probes (BioRad, Hercules, USA).

550 Nasal conchae samples from ferret #3 and #4 were subjected to high-throughput sequencing  
551 and viral genomes compared to the inoculum (study accession number: PRJEB37671) by  
552 employing previously published high throughput sequencing procedures using Ion Torrent  
553 S5XL instrument (29).

#### 554 Detection of SARS-CoV-2 reactive antibodies

555 Serum samples collected before the start of the experiments as well as on necropsy were tested  
556 for the presence of SARS-CoV-2 reactive antibodies by indirect immunofluorescence assay  
557 (iIFA) and virus neutralization test (VNT).

558 Confluent Vero E6 cells in a 96 well plate were infected with 0.1 MOI of SARS-CoV-2 or cell  
559 culture medium for negative control cells. After 24h, cells were fixed with 4%  
560 paraformaldehyde and permeabilized with 0.5% Triton-X-100. Serum samples were heat  
561 inactivated at 56°C for 30 min. For antibody detection, 50 µl of a 2-fold dilution series of the  
562 serum samples (starting from 1:20) were added in parallel to the SARS-CoV-2 positive and  
563 negative cells. After 1h incubation, cells were washed and incubated for 1h with a goat-anti-  
564 ferret-IgG-FITC antibody (1:250, Bethyl, Texas, USA), mouse-anti-bat-IgG #6 (1:100, FLI  
565 produced) combined with a goat-anti-mouse-Cy3 (1:400, Jackson Immunoresearch,  
566 Pennsylvania, USA), goat-anti-pig-FITC IgG (1:2000, antibodies-online, Aachen, Germany),  
567 goat-anti-chicken-IgG-FITC (1:400, OriGene Technologies GmbH, Maryland, USA),  
568 respectively. After final washing, cells were analyzed by fluorescence microscopy.

569 For virus neutralization assay, 50 µl of medium containing  $10^{3.3}$  TCID<sub>50</sub> SARS-CoV-2 were  
570 mixed with 50 µl of diluted serum. Each sample was tested in triplicates. After 1h incubation  
571 at 37°C the mixture was transferred to confluent Vero E6 cells in a 96 well plate. Viral  
572 replication was assessed after 5 days at 37°C, 5% CO<sub>2</sub> by the detection of CPE.

#### 573 Virus titration

574 Virus titer used for infection experiments was confirmed by titration on Vero E6 cells and  
575 evaluation of CPE after 5 days. RT-qPCR positive nasal washes and tissue samples were titrated  
576 on Vero E6 cells as well.

#### 577 Pathology: Necropsy, histopathology, immunohistochemistry, in situ hybridization

578 Full necropsies were performed on all animals according to a standard protocol under BSL3  
579 conditions. The following tissues were collected and fixed in 10% neutral-buffered formalin:  
580 Nasal conchae (non-respiratory, respiratory and olfactory region), trachea, lung (inflated with  
581 formalin, left and right cranial as well as caudal lobe), tracheobronchial lymph node, heart (left  
582 ventricle), liver, spleen, duodenum, colon, pancreas, kidney, adrenal gland, skeletal muscle,  
583 skin, brain. Tissues of ferrets and fruit bats were embedded in paraffin, and 3 µm sections were  
584 stained with hematoxylin and eosin for light microscopical examination.

585 For SARS-CoV-2 antigen detection, tissue sections of all bats and ferrets were deparaffinized  
586 and rehydrated according to standardized procedures. Antigen heat retrieval was performed  
587 (citrate buffer, pH 6, 12 min, microwave 600 Watt). Nonspecific antibody binding was blocked  
588 with goat normal serum for 30 min at room temperature. Polyclonal rabbit anti SARS-CoV-2  
589 antibody (dilution 1:200, Novus Biologicals # NB100-56576, Centennial, CO, USA) was  
590 incubated over night at room temperature, followed by washing steps and incubation with a  
591 secondary biotinylated goat anti-rabbit antibody (dilution 1:200; Vector Laboratories,  
592 Burlingame, CA, USA) for 30 min at room temperature. Freshly prepared avidin-biotin-  
593 peroxidase complex (ABC) solution (Vectastain Elite ABC Kit; Vector Laboratories) was  
594 applied, and a bright red antigen labelling was produced with the 3-amino-9-ethylcarbazole  
595 substrate (AEC, Dako, Agilent, Santa Clara, CA, USA). The sections were counterstained with  
596 hematoxylin, rehydrated, and mounted on coverslips. In each run, we included consecutive  
597 sections incubated with negative rabbit control serum, historical tissue sections from SARS-  
598 CoV-2 negative ferrets and bats (negative control), and sections of cell pellets infected with  
599 SARS-CoV-2 and fixed after 24 h (positive control).

600 To confirm IHC, RNA in situ hybridization (ISH) was performed on tissues of selected animals  
601 with RNAScope 2-5 HD Reagent Kit-Red (ACD, Advanced Cell Diagnostics, Newark, CA)  
602 according to the manufacturer's instructions. For hybridization, RNAScope® probes were  
603 custom designed by ACD for SARS-CoV-2 NSP. The specificity of the probes was verified  
604 using a positive control probe peptidylprolyl isomerase B (cyclophilin B, ppib) and a negative  
605 control probe dihydrodipicolinate reductase (DapB). Evaluation and interpretation of pathology  
606 data were performed by a board-certified pathologist (DiplECVP).

#### 607 Susceptibility of different porcine cell lines to SARS-CoV-2

608 Porcine cell lines, porcine kidney-15 (PK-15), swine kidney-6 (SK-6) and swine testicle (ST)  
609 cells that are routinely used for porcine virus isolation attempts at FLI, were investigated for  
610 their permissivity to SARS-CoV-2. Cells were maintained in modified Eagle medium (MEM)

611 supplemented with 10% FBS. Nearly confluent cells were infected with SARS-CoV-2 at a titer  
612 of  $10^{5.5}$  TCID<sub>50</sub> in a microtitration format in 96well plates or were mock-infected with medium  
613 only. Vero E6 cells were used as a highly permissive control. Cells were observed for cytopathic  
614 effects (CPE) daily until six days post infection.

615 Susceptibility of embryonated chicken eggs

616 Six 9-day-old SPF chicken eggs were inoculated by allantoic sac route, using 0.1 ml with  
617  $5.5 \times 10^4$  TCID<sub>50</sub>. Amniotic-Allantoic fluid (AAF) was harvested after incubation for 7 days and  
618 tested by RT-qPCR and virus isolation on Vero E6 cells.

619

620

621 **Supplementary Tables**

622 **Table S1: Histopathologic findings in the lungs of inoculated and contact Egyptian fruit**  
 623 **bats and ferrets.** For all animals, the left and right, cranial as well as caudal lung lobes (= 4 in  
 624 total) were examined.

	Infiltrates, interstitial, mixed, mild	Infiltrates, perivascular, lymphocytic, mild	Infiltrates, intra alveolar, mixed, minimal	Alveolar macrophages, number increased, minimal
Day 4	Bat#1; 4/4 lobes			Bat#2; 1/4 lobes
	Ferret#2; 1/4 lobes	Ferret#2; 4/4 lobes	Ferret#1, #2; 1/4 lobes	Ferret#1, 2/4 lobes, Ferret#2; 3/4 lobes
Day 8	Bat#4; 1/4 lobes			
	Ferret#3; 3/4 lobes	Ferret#3; 1/4 lobes		Ferret#3, 4; 1/4 lobes
Day 12	Bat#5; 2/4 lobes			
				Ferret#6; 2/4 lobes
Day 21				Bat#7, 8; 1/4 lobes
				Ferret#8; 1/4 lobes
Day 21 Contact	Bat#10; 1/4 lobes	Bat#10; 1/4 lobes		Bat#10; 2/4 lobes, Bat #11; 1/4 lobes
	Ferret#10, 11; 4/4 lobes, Ferret#12, 11; 1/4 lobes	Ferret#10; 3/4 lobes		Ferret#10, 12 3/4 lobes; Ferret#11, 1/4 lobes;

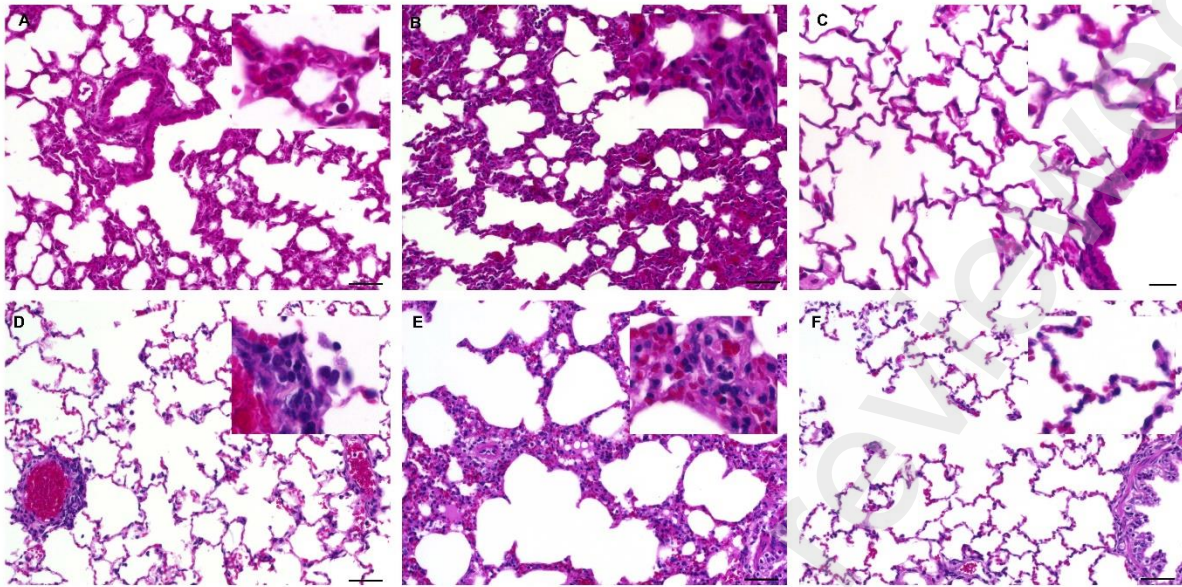
625

626

627

628

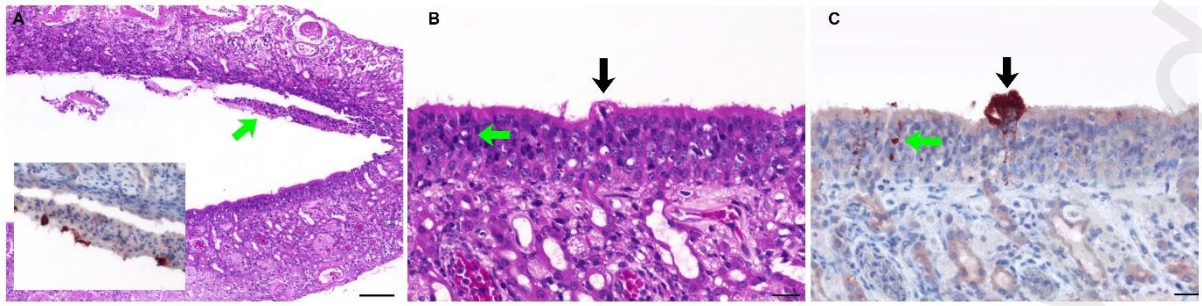
629 **Supplementary Figures**



630

631 **Figure S1: SARS-CoV-2 associated pulmonary lesions in bats (A-C) and ferrets (D-F).** (A)  
632 Thickening of the alveolar wall by congestion and slight, neutrophilic infiltrates, bat, day 4 pi,  
633 bar 50  $\mu\text{m}$  (B) Pronounced thickening by congestion and mixed cellular infiltration of the  
634 alveolar wall, contact bat, day 21, bar 50  $\mu\text{m}$ , (C) No relevant findings in inoculated bats at day  
635 21 pi, bar 50  $\mu\text{m}$  (D) Perivascular, mononuclear infiltrates, ferret, day 4, bar 50  $\mu\text{m}$ , (E)  
636 Thickening by congestion and infiltration of the alveolar wall, contact ferret, day 21, bar 50  
637  $\mu\text{m}$ , (F) No relevant findings in inoculated ferrets at day 21 pi, bar 50  $\mu\text{m}$ .

638

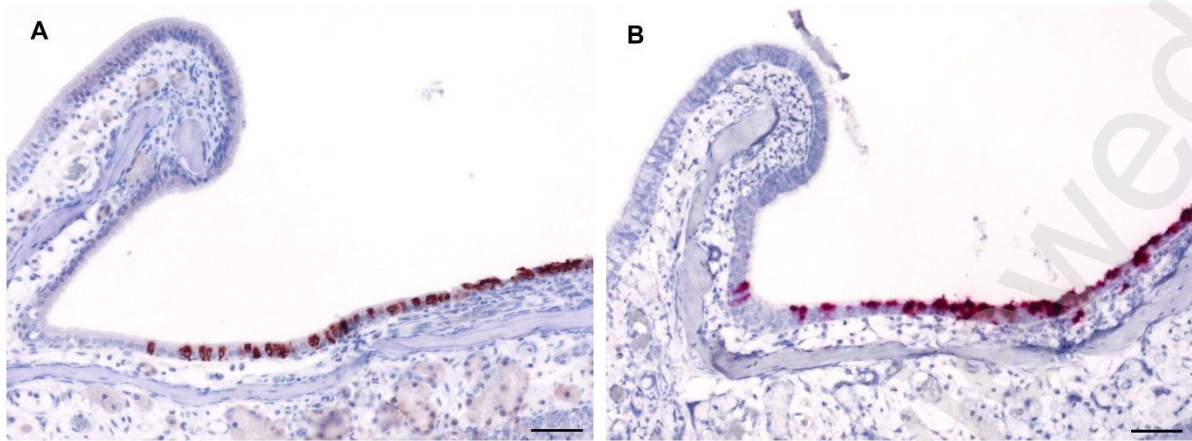


639

640 **Figure S2: SARS-CoV-2 in the vomero-nasal organ of a contact ferret on day 21.** (A)  
641 Intraluminal debris (green arrow), extensive degeneration, necrosis and focal loss of the  
642 olfactory epithelium, abundant mixed cellular infiltrates, intralesional viral antigen (inlay), bar  
643 100  $\mu\text{m}$ , (B) Degeneration with swelling of the olfactory epithelium (black arrow) and apoptosis  
644 (green arrow), bar 20  $\mu\text{m}$ , consecutive slide (C) Viral antigen within olfactory epithelium (black  
645 and green arrow), bar 20  $\mu\text{m}$ . (A, B) H&E stain, (inlay and C) Immunohistochemistry, ABC  
646 Method, AEC chromogen (red-brown), Mayer's hematoxylin counter stain (blue), bar 20  $\mu\text{m}$ .

647

648



649

650 **Figure S3: Comparative SARS-CoV-2 antigen and RNA detection.** Immunohistochemistry  
651 and in situ hybridization yielded comparative results with respect to cell types affected and  
652 semi-quantitative antigen amount. Exemplarily shown in the respiratory epithelium, ferret, 4  
653 dpi. (A) Immunohistochemistry, ABC Method, AEC chromogen (red-brown), Mayer's  
654 hematoxylin counter stain (blue), (B) In situ hybridization, RNAScope®, chromogenic  
655 labelling (fast red) with probes to SARS-Cov-2 NSP, Mayer's hematoxylin counter stain (blue).

656

657

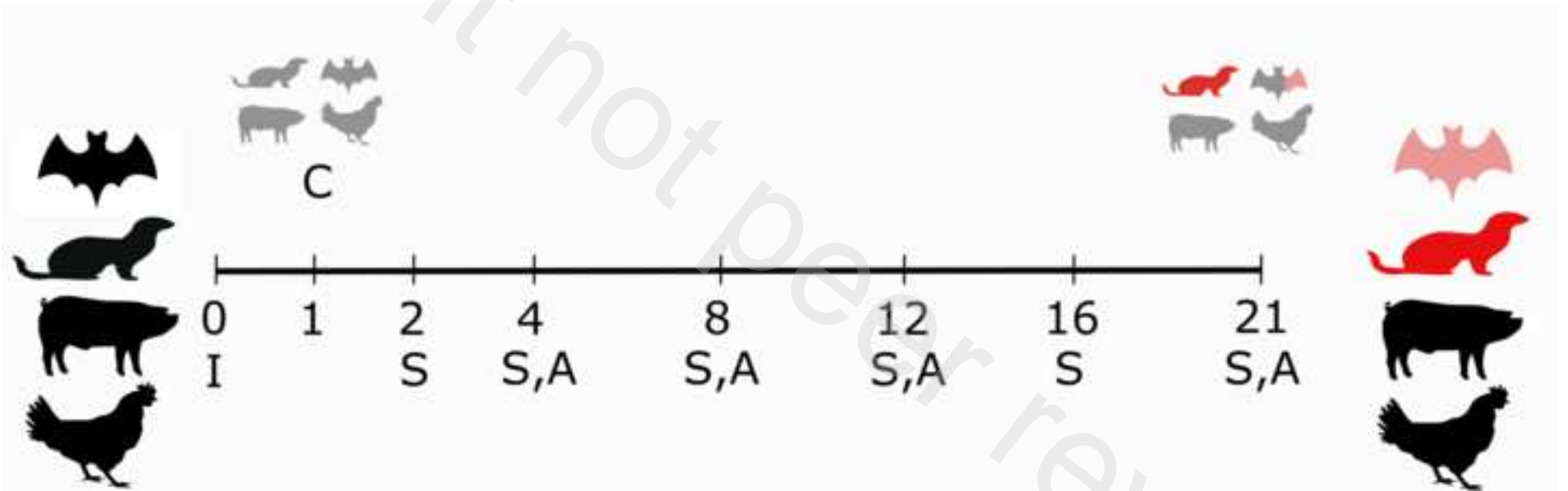
658

659

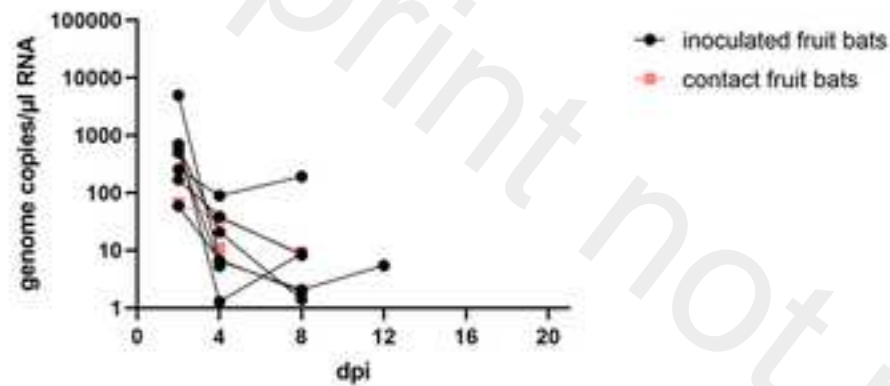
660

661

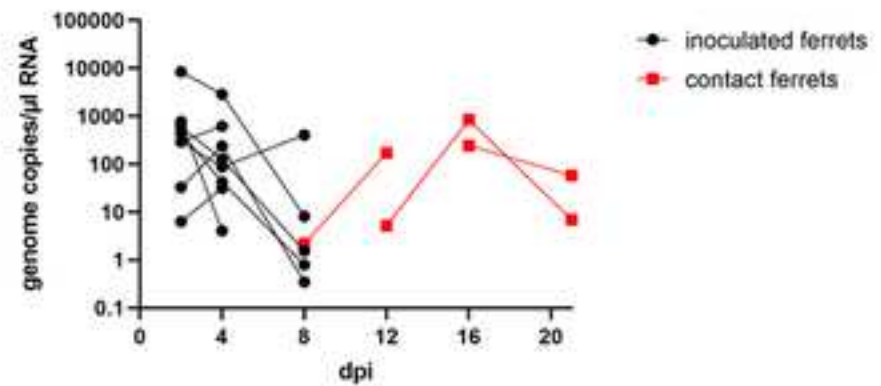




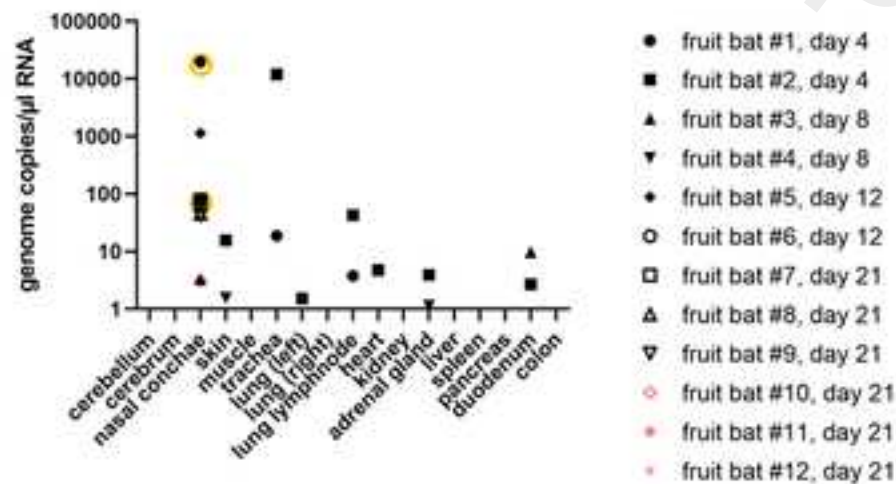
A) Viral load fruit bat oral swabs



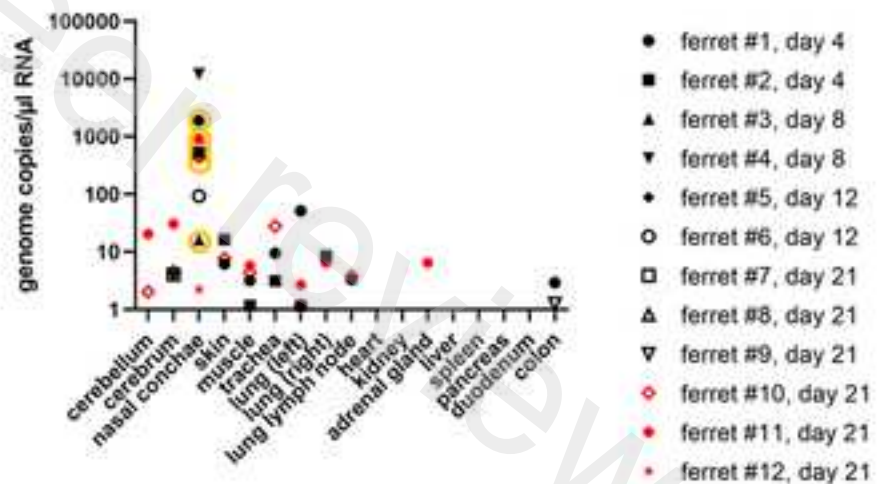
B) Viral load ferret nasal washes

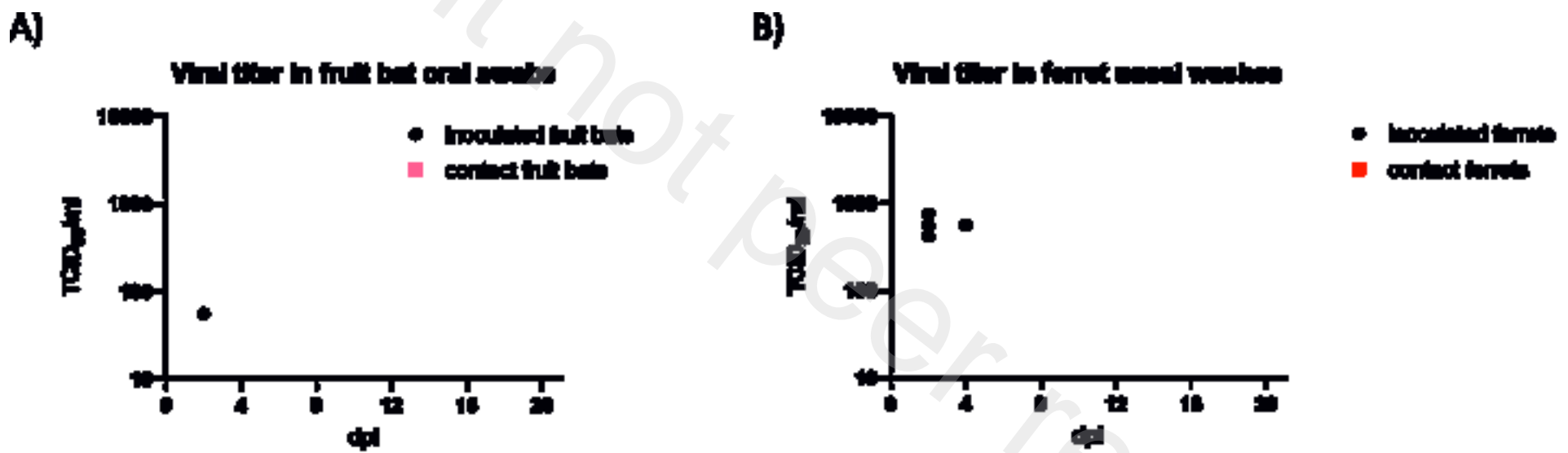


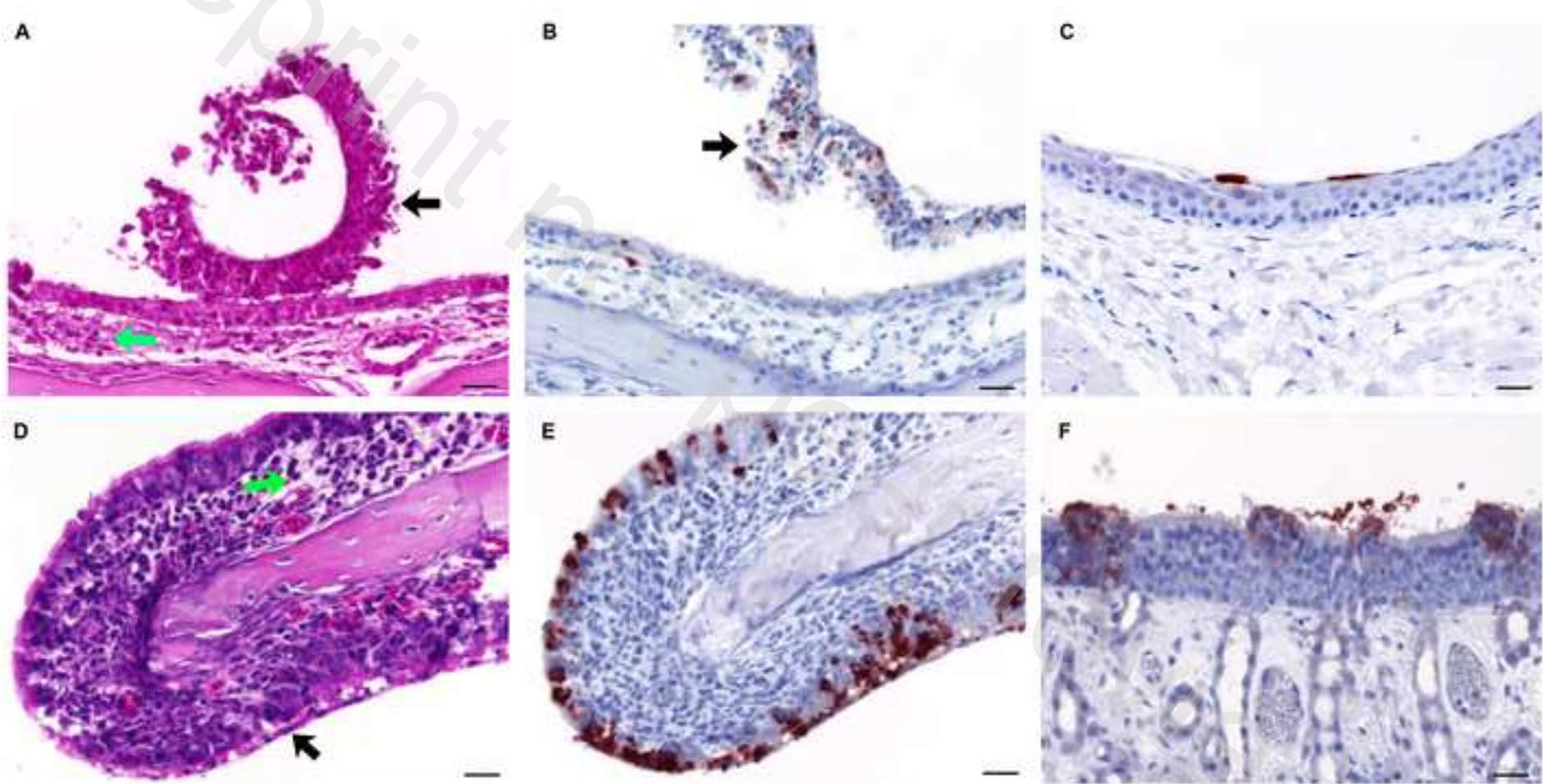
C) Viral load fruit bat tissues

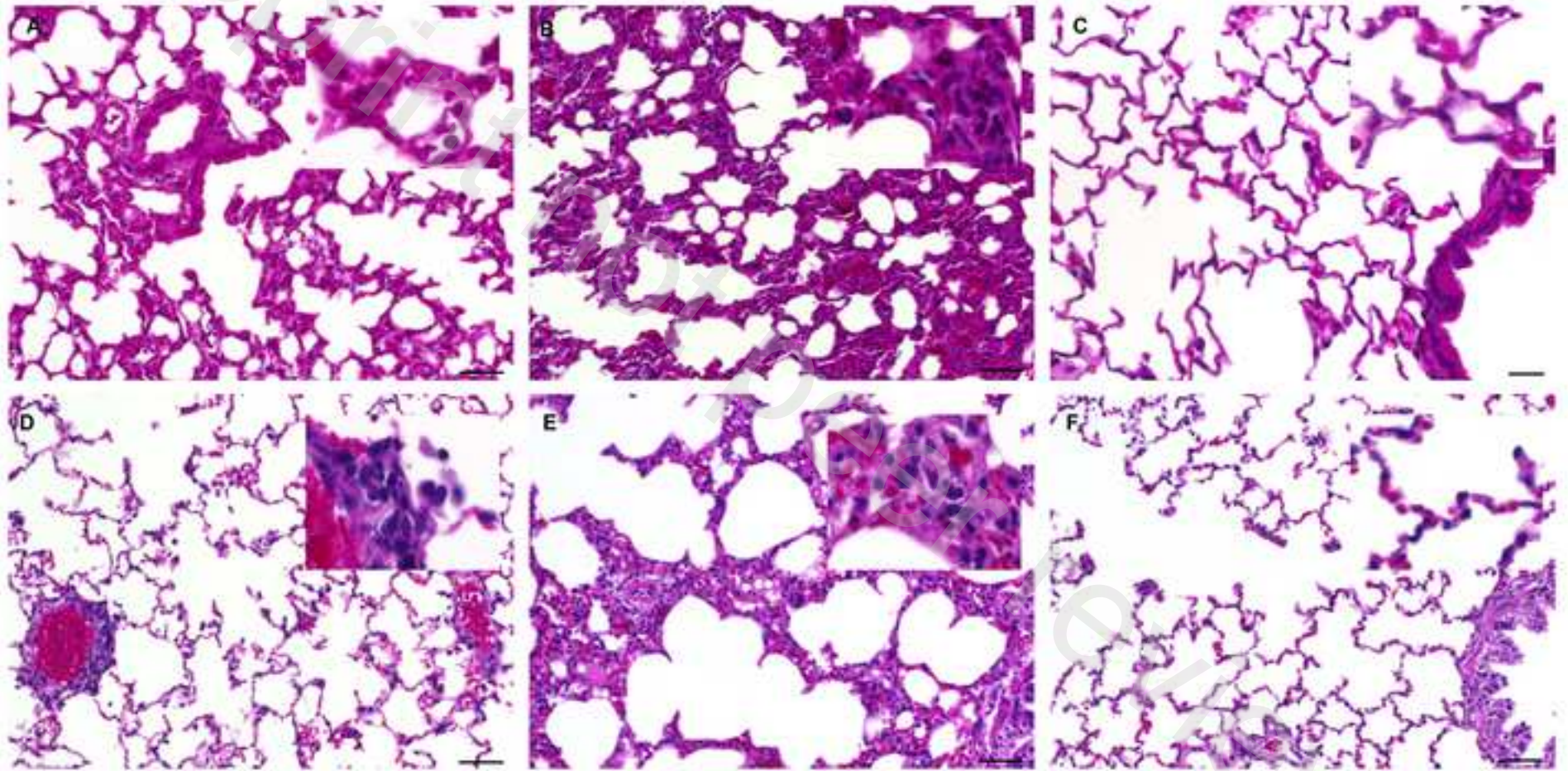


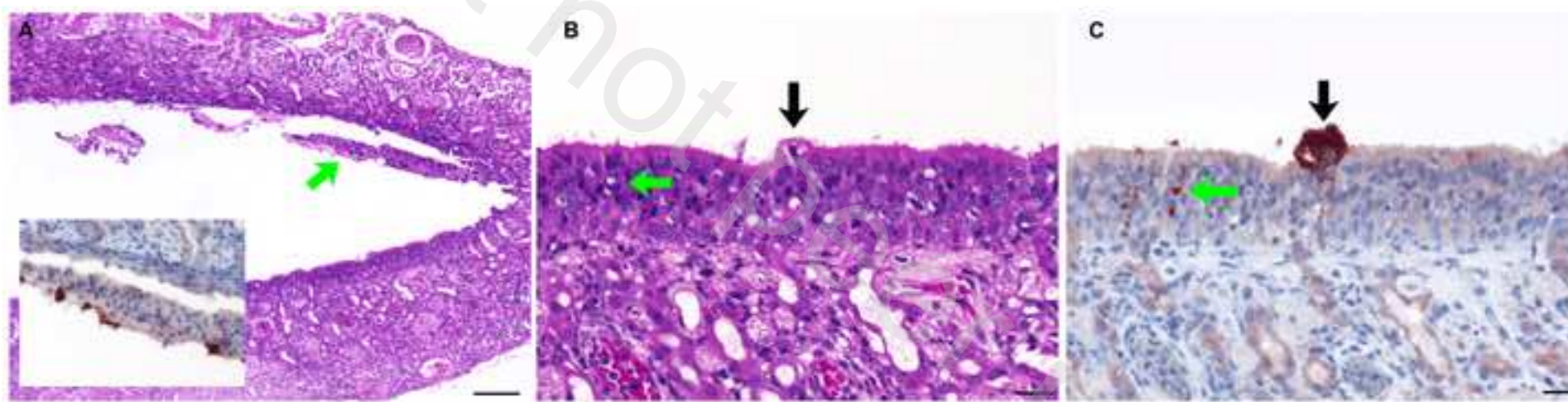
D) Viral load ferret tissue



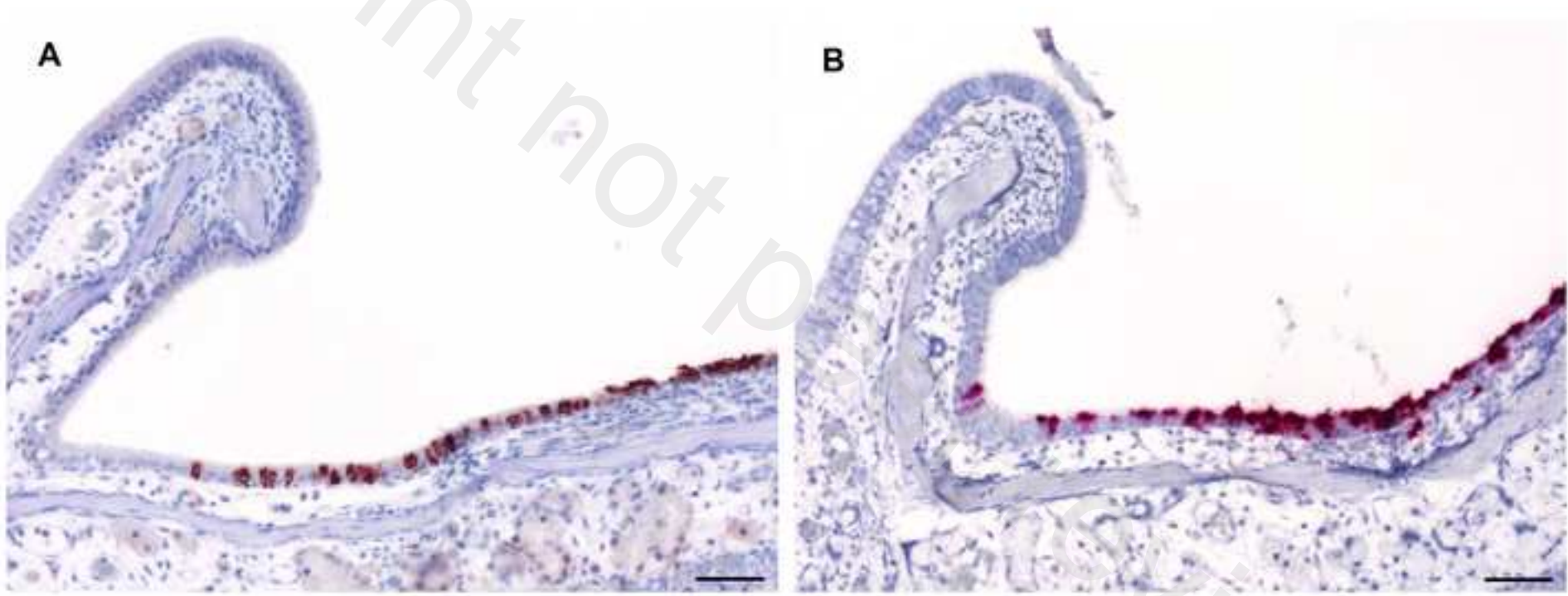








reviewed



Preprint not peer reviewed